UAV Assisted Integrated Sensing and Communications for Internet of Things: 3D Trajectory Optimization And Resource Allocation

Zechen Liu, Xin Liu, *Senior Member, IEEE,* Yuemin Liu, Victor C. M. Leung, *Life Fellow, IEEE,* and Tariq S. Durrani, *Life Fellow, IEEE*

***Abstract*—High-mobility unmanned aerial vehicles (UAVs) can serve as dual-function aerial service platforms for the Internet of Things (IoT), providing both sensing and communication services for IoT nodes without a base station (BS), particularly in emergency situations. In this paper, a UAV-assisted integrated sensing and communications (ISAC) system is proposed for IoT, which simultaneously senses the status information around the IoT and sends the sensing information to both the IoT nodes and a data collection center. In order to assess the sensing performance of ISAC, the radar estimation rate is introduced as a significant metric from the perspective of information theory. Considering the mutual interference between sensing and communications, the radar estimation rate is maximized through the coordinated optimization of UAV task scheduling, transmit power allocation, and 3D flight parameters under the constraint of communication rate. The formulated non-convex mixed-integer programming problem is divided into three subproblems, including UAV task scheduling optimization, UAV sensing and communication power optimization, and UAV 3D flight parameters optimization. The optimal solutions can be achieved by proposing a three-layer iterative optimization algorithm to optimize the three subproblems iteratively. The simulation results show that the radar estimation rate can well measure the sensing performance of the ISAC, which can be effectively improved by optimizing the 3D UAV flight parameters.**

***Index Terms*—UAV, ISAC, IoT, radar estimation rate, resource allocation, 3D flight trajectory optimization.**

I. Introduction

Internet of Things (IoT) has emerged as a crucial information network that seamlessly integrates the physical and digital worlds through sensing and communication in various fields, such as agriculture, healthcare, and transportation, etc [1]-[3]. By erecting IoT Gateway and base stations (BSs), the IoT nodes can acquire and share environmental information with surrounding devices, infrastructures, and pedestrians [4]-[6]. However, when the number of nodes is large or the BSs are lacking, the IoT cannot efficiently exchange information [7]-[10]. To solve this problem, unmanned aerial vehicles (UAVs) are adopted as aerial platforms to assist ground IoT communications. The aerial communication link between the UAV and ground nodes is much better than the ground communication link and can be seen as line-of-sight (LoS). Meanwhile, due to its high mobility, the UAV is very suitable for assisting IoT in remote areas or emergency scenarios [11]. To realize communication and sensing for IoT, the UAV needs to load communication and sensing devices separately, which will increase the load and spectrum consumption of the UAV. Fortunately, integrated sensing and communications (ISAC) technology is currently being developed to reduce equipment redundancy and improve spectrum utilization, which is regarded as one of the significant research directions for IoT in the future [12]-[15].

During the development of ISAC technology, radar and communication signals are emitted by one transmitter and will gradually merge, eventually sharing spectrum and signal processing equipment. Thus, equipment redundancy is reduced and spectrum utilization is improved. In [16], Chiriyath *et al.* proposed an evaluation criterion for radar estimation rate based on the Cramer-Rao bound (CRB) and introduced a theoretical evaluation criterion for the joint radar and communication system. In [17], Liu *et al.* proposed a dual-functional radar-communication (DFRC) system, where a transmitter detects the radar target and communicates with downlink users simultaneously. The downlink mutual interference was minimized by considering omnidirectional and directional beampattern design. In [18], a full-duplex (FD) ISAC scheme was proposed by Xiao *et al.*, where the waiting time of pulsed radars was utilized for transmitting communication signals. In [19], a multibeam architecture using controllable antenna arrays was proposed by zhang *et al.*, where the sensing and communication could be seamlessly integrated. In [20], a wireless scheduling framework was proposed by Zhao *et al.*, where the Cobb-Douglas utility function was maximized by jointly optimizing the coordination gains of communication, computation and sensing. In [21], Zhao *et al.* proposed a dual-function BS model in the signal correlated interference scenario, where the design of receive and transmit beamforming vectors is to ensure a balance between communication and radar in imperfect and perfect channels. In [22], a RUs assisted vehicular communication system was proposed by Yuan *et al.*, where the ISAC technology was used to assist orthogonal time

This work was supported by the Xi'an Key Laboratory of Network Convergence Communication under Grant 2022NCC-K101. *(Correspondence author: Xin Liu.)*

Zechen Liu, Xin Liu and Yuemin Liu are with the School of Information and Communication Engineering, Dalian University of Technology, Dalian 116024, China (e-mail: liuxinstar1984@dlut.edu.cn; lzc_sdzb@mail.dlut.edu.cn; 6ym@mail.dlut.edu.cn).

Victor C. M. Leung is with the College of Computer Science and Software Engineering, Shenzhen University, Shenzhen, China 518060 (e-mail: vleung@ieee.org).

Tariq S. Durrani is with the Department of Electronic and Electrical Engineering, University of Strathclyde, Glasgow G1 1XQ, U.K. (e-mail: t.durrani@strath.ac.uk).

This is a peer-reviewed, accepted manuscript of the following paper: Liu, Z., Liu, X., Liu, Y., Leung, V. C. M., & Durrani, T. S. (2024). UAV assisted integrated sensing and communications for Internet of Things: 3D trajectory optimization and resource allocation. IEEE Transactions on Wireless Communications. Advance online publication. https://doi.org/10.1109/TWC.2024.3352985

frequency space (OTFS) transmission in bidirectional link. In [23], Mu *et al.* proposed a high-mobility vehicular network, where the estimation error caused by nonlinear measurements was reduced by leveraging deep learning method to estimate the angle. In [24], a dynamic frame structure configuration of dual-function IoV network based on 5G new wireless protocol was proposed by Zhang *et al.*, and the optimal percentage of time duration allocation was obtained by maximizing the radar mutual information (MI). In [25], Zhang *et al.* proposed a time division based ISAC model for connected automated vehicles (CAVs), where the closed-form solution for the vehicle-to-everything (V2X) cooperative communication mode selection was obtained by the mmWave enabled CAVs cooperation algorithm.

The above studies mainly consider ISAC applications in the ground layer. However, ISAC will not work effectively when ground infrastructures are lacking or paralyzed. Meanwhile, the high cost of ground infrastructure also determines that it cannot be deployed on a large scale in the remote areas. Therefore, deploying an ISAC system on the UAV holds significant practical significance. In [26], Jiang *et al.* proposed a UAV swarm wireless network, in which the accuracy of target sensing was improved by the extended kalman filter method and the delay of communication was reduced by Identification Friend or Foe algorithm. In [27], Chang *et al.* proposed a joint scheduling strategy for control, communication and sensing of mmWave communications in UAV network. The authors used state-noise-ratio to denote the relationship between beam alignment and sensing-control pattern, and obtained a closed-form expression for the design of data rate triggered sensing-control pattern. In [28], a dual-function multi-UAV wireless network was proposed by Wang *et al.*, where the utility of network was maximized by jointly optimizing UAV location, UAV transmit power, and user association under the localization accuracy constraint. In [29], a cooperative sensing UAV system was proposed by Chen *et al.*, where the UAV simultaneously conducted radar detection and sensing information fusion communication. The performance of collaborative sensing was enhanced by optimizing the upper-bound of the proposed average cooperative sensing area.

The aforementioned researches mainly discuss the ISAC in the static UAV and ignore the movement of the UAV. To further exploit the advantage of UAV mobility, a few literatures have considered the ISAC applications in mobile UAV scenarios. In [30], a UAV aided ISAC network was proposed by Zhang *et al.*, where the peak age of information (AoI) of the UAV-ISAC system was minimized by optimizing UAV power, scheduling order, trajectory and time allocation for both communication and sensing. In [31], Zhang *et al.* proposed a dual-function UAV cellular network, where the AoI determined by UAV sensing and transmission was minimized by jointly optimizing sensing time, transmission time, task scheduling and UAV trajectory. In [32], Hu *et al.* proposed a novel base station (BS)-UAV enabled bistatic synthetic aperture radar (SAR) platform to perform communication-assisted radar sensing, where the UAV propulsion consumption was minimized by planning the flight trajectory under the constraint of radar resolution. In [33], a multi-UAV enabled integrated radar and communication system was proposed by Zhang *et al.*, where the sensing performance and fairness were both maximized by optimizing navigation, transmit power and resource allocation through deep reinforcement learning method. In [34], a UAV assisted periodic communication and sensing scheme was proposed by Meng *et al.*, where the penalty-based algorithm was utilized to maximize the achievable rate by iteratively optimizing sensing time allocation, user association, UAV trajectory and beamforming vector. In [35], a UAV assisted ISAC system was proposed by Liu *et al.*, where the minimum radar MI and the UAV energy efficiency were simultaneously maximized by optimizing UAV transmit power, scheduling and trajectory. However, [30] and [31] only considered to improve the communication performance, but overlooked the sensing performance, an important indicator for ISAC. [32]-[35] only focused on optimizing the 2D trajectory of the UAV assisted ISAC, but ignored the potential performance gain brought by optimizing the 3D UAV trajectory.

In this paper, a UAV assisted ISAC model is proposed for IoT, in which the UAV is deployed as a dual-function aerial platform to provide sensing and communication services for the ground IoT nodes. The radar estimation rate of the UAV assisted ISAC is maximized by considering both the performance metric of radar detection and the dynamic 3D trajectory of the UAV. The contributions of this paper are summarized as follow.

- A UAV-enabled ISAC model is established, in which the UAV flies over the target area to perform ISAC and data upload tasks. We introduce the radar estimation rate as a metric to evaluate the sensing performance of radar detection in ISAC from the information theory perspective.
- We formulate an efficient optimization problem to maximize the radar estimation rate by jointly optimizing UAV task scheduling, transmit power allocation and 3D flight parameters. Specifically, we consider the mutual interference of communication and sensing in the resource allocation, which has a great impact on an actual ISAC system.
- The complex mix-integer initial optimization problem is divided into three parts: task scheduling optimization, sensing and communication power optimization and 3D flight parameters optimization. Based on the successive convex approximation (SCA) method, we propose a three-layer iterative optimization algorithm to get the optimal solution to the initial problem.

The rest of this paper is organized as follows. In Section II, we propose a UAV-assisted ISAC model for IoT, and by introducing the radar estimation rate to evaluate the sensing performance of ISAC, we formulate an optimization problem to maximize the radar estimation rate. In Section III, a three-layer iterative optimization algorithm is proposed to solve the initial optimization problem. In Section IV, some numerical simulation results are presented and analyzed. In Section V, we conclude the paper and indicate the future research directions.

This is a peer-reviewed, accepted manuscript of the following paper: Liu, Z., Liu, X., Liu, Y., Leung, V. C. M., & Durrani, T. S. (2024). UAV assisted integrated sensing and communications for Internet of Things: 3D trajectory optimization and resource allocation. IEEE Transactions on Wireless Communications. Advance online publication. https://doi.org/10.1109/TWC.2024.3352985

II. System Model And Problem Formulation

In this section, we will first provide a brief introduction to the proposed UAV assisted ISAC system. Then, we will introduce two metrics for measuring communication and sensing performance of the ISAC system. Finally, we will transform the proposed system model into a mathematical optimization problem. For ease of reference, we provide a list of the notations used in this paper in Table I.

TABLE I
Summary of Notations

Symbol	Meaning
K	number of IoT nodes
T	flight cycle time
Q	number of time slots
B	signal bandwidth
Δt	length of one time slot
$\mathbf{g}_c$	location of data collection center
$\mathbf{g}_k$	location of the IoT node k
$\mathbf{g}_u(q)$	location of the UAV in time slot q
$H_u^{\min}$	minimum UAV flight height
$H_u^{\max}$	maximum UAV flight height
v_{xy}	horizontal flight speed of the UAV
v_z	vertical flight speed of the UAV
$v_{xy}^{\max}$	maximum horizontal flight speed of the UAV
$v_z^{\max}$	maximum vertical flight speed of the UAV
$a_{xy}^{\max}$	maximum UAV horizontal acceleration
$a_z^{\max}$	maximum UAV vertical acceleration
$\mathbf{v}(q)$	UAV flight speed
θ	maximum UAV detection angle
$\omega_k(q)$	ISAC task index
$b(q)$	data upload task index
G_t	antenna gain of the UAV transmitter
G_r	antenna gain of the UAV receiver
G_c	antenna gain of the data collection center receiver
d_c	distance between the data collection center and UAV
d_k	distance between the IoT node k and UAV
λ	signal wavelength
f_c	signal carrier frequency
c	speed of light
$P_t(q)$	transmit power of the UAV in time slot q
$P_{rad}(q)$	sensing power of the UAV in time slot q
$P_{com}(q)$	communicaton power of the UAV in time slot q
$\alpha(q)$	power allocation factor
$h_{k,com}(q)$	communication channel power gain in time slot q
$h_{k,rad}(q)$	radar channel power gain in time slot q
$\Gamma_{k,com}(q)$	SINR of communication channel in time slot q
$\Gamma_{k,rad}(q)$	SINR of radar channel in time slot q

A. Scenario Description

As shown in Fig. 1, we consider a dual function UAV-assisted IoT system consisting of a UAV, a data collection center, and several IoT nodes. The UAV with ISAC function is deployed to serve K IoT nodes with impaired sensing capabilities and transmit the sensing information to the data collection center.[1] Let $k \in \mathcal{K} = \{1, 2, ..., K\}$ denote the index of ground IoT nodes, which are randomly distributed around the data collection center.[2] Let $\mathbf{g}_c = [l_c \ H_c]$ and $\mathbf{g}_k = [l_k \ H_k]$ denote the fixed locations of the data collection center and IoT nodes, where $l_c = [x_c, y_c]$ and $l_k = [x_k, y_k]$ denote the horizontal positions of data collection center and IoT nodes, respectively, while H_c and H_k represent the altitudes of data collection center and IoT nodes, respectively.

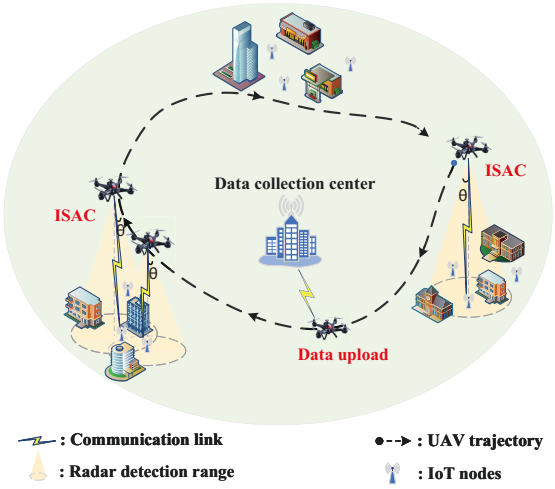

Fig. 1. System model.

We consider that the UAV flies over the target area with constant flight cycle and varying flight altitude to perform ISAC and data upload tasks. When a node is within the detection range of the UAV radar, the UAV will perform the ISAC task, that is, simultaneously sending a radar signal to sense the status information around the node and forwarding a communication signal containing the sensed information to the corresponding node. When the nodes are out of the detection range of the UAV radar, the UAV will execute the data upload task, that is, sending the stored sensing information to the data collection center through the communication uplink.

In order to make a reasonable analysis of the system, time discretization (TD) method is adopted to discrete the UAV flight trajectory. We make a assumption that the total flight time T can be decomposed into Q time slots with the same time interval of $\Delta t = T/Q$. Specifically, Δt needs to be small enough so that the UAV trajectory can be approximated as a short straight line in each time slot. Hence, the 3D coordinate of the UAV can be denoted as $\mathbf{g}_u(q) = [l_u(q) \ H_u(q)]$, where $q \in \mathcal{Q} = \{1, 2, \ldots, Q\}$, $l_u(q) = [x_u(q), y_u(q)]$ and $H_u(q)$ denote the real time horizontal position and flight altitude of the UAV, respectively. Furthermore, in order to ensure that the UAV has a continuous and smooth flight cycle, the UAV trajectory should satisfy the mobility constraints, meanwhile, the initial and end states of the UAV should be the same. These constraints can be denoted as

$$l_u(q+1) = l_u(q) + v_{xy}(q)\Delta t, \forall q \tag{1}$$

[1]Under the normal circumstances, the IoT node has the ability to transmit its status information to the data collection center. However, under the harsh circumstances, the communication link between the IoT node and the data collection center may be interrupted, resulting in the loss of node information. In such cases, it is crucial to utilize the UAV to provide emergency ISAC services for the IoT nodes.

[2]Here, we make the assumption that the locations of both the IoT nodes and data collection center are fixed, and known to the UAV. This scenario is commonly encountered in practical settings. For example, in data collection scenarios, the UAV can be programmed to efficiently navigate and collect sensing information from pre-deployed IoT nodes.

This is a peer-reviewed, accepted manuscript of the following paper: Liu, Z., Liu, X., Liu, Y., Leung, V. C. M., & Durrani, T. S. (2024). UAV assisted integrated sensing and communications for Internet of Things: 3D trajectory optimization and resource allocation. IEEE Transactions on Wireless Communications. Advance online publication. https://doi.org/10.1109/TWC.2024.3352985

$$H_u(q+1) = H_u(q) + v_z(q)\Delta t, \forall q \tag{2}$$

$$\|v_{xy}(q+1) - v_{xy}(q)\| \leq a_{xy}^{\max}, \forall q \tag{3}$$

$$\|v_z(q+1) - v_z(q)\| \leq a_z^{\max}, \forall q \tag{4}$$

$$\mathbf{v}(1) = \mathbf{v}(Q) \tag{5}$$

$$\mathbf{g}_u(1) = \mathbf{g}_u(Q) \tag{6}$$

where $v_{xy}(q)$ and $v_z(q)$ denote the horizontal and vertical speeds of the UAV at time slot q, respectively; $\|\bullet\|$ represents the L_2 norm, $a_{xy}^{\max}$ and $a_z^{\max}$ indicate the maximum horizontal and vertical accelerations of the UAV, respectively; $\mathbf{v}(q) = [v_{xy}(q)\ v_z(q)]$ denotes the UAV flight speed in 3D space.

For convenience, we introduce two discrete binary variables, $\omega_k(q)$ and $b(q)$, to indicate the scheduling of the ISAC and data upload tasks. We assume that the UAV can only perform one kind of task on one node or data collection center per time slot. When the UAV performs the ISAC task on the IoT node k at time slot q, we set $\omega_k(q) = 1$ and $b(q) = 0$. When the UAV performs the data upload task for data collection center, we set $\omega_k(q) = 0$ and $b(q) = 1$. Hence, the constraints for $\omega_k(q)$ and $b(q)$ can be written as

$$\omega_k(q) \in \{0,1\}, \forall k, q \tag{7}$$

$$b(q) \in \{0,1\}, \forall q \tag{8}$$

$$\sum_{k=1}^{K} \omega_k(q) + b(q) = 1, \forall q \tag{9}$$

Without loss of generality, we define θ as the maximum detection angle of the UAV.[3] To execute the ISAC task, the detection range of the UAV should cover the target node, hence, the location constraint for the UAV can be given as

$$\omega_k(q)\Big((x_u(q) - x_k)^2 + (y_u(q) - y_k)^2\Big) \leq (H_u(q)\tan\theta)^2, \forall k, q \tag{10}$$

Compared with the ground communication links, the aerial channel links from the UAV to the data collection center and IoT nodes are dominated by the LoS link. [4] Therefore, the power gain of the communication link from UAV to data collection center and node k at time slot q can be expressed as [42]

$$h_c(q) = \frac{G_t G_c \lambda^2}{(4\pi)^2 d_c^2(q)} = \frac{\beta_{com}}{d_c^2(q)}, \forall q \tag{11}$$

$$h_{k,com}(q) = \frac{G_t G_c \lambda^2}{(4\pi)^2 d_k^2(q)} = \frac{\beta_{com}}{d_k^2(q)}, \forall k, q \tag{12}$$

where G_c and G_t denote the antenna gains of the UAV transmitter and communication receiver, respectively; $\lambda = c/f_c$ indicates the signal wavelength, where c and f_c denote the speed of light and signal carrier frequency, respectively; $d_c(q) = \|\mathbf{g}_u(q) - \mathbf{g}_c\|$ and $d_k(q) = \|\mathbf{g}_u(q) - \mathbf{g}_k\|$ represent the distance from the UAV to the data collection center and node k, respectively; $\beta_{com} = \frac{G_t G_c \lambda^2}{(4\pi)^2}$.

Considering both the transmission and echo links of radar signal [43], the power gain of the radar detection link between the UAV and the node k at time slot q can be denoted as

$$h_{k,rad}(q) = \frac{G_t G_r \lambda^2 \sigma}{(4\pi)^3 d_k^4(q)} = \frac{\beta_{rad}}{d_k^4(q)}, \forall k, q \tag{13}$$

where G_r denotes the antenna gain of UAV radar receiver, and σ denotes radar cross-section (RCS) of the target; $\beta_{rad} = \frac{G_t G_r \lambda^2 \sigma}{(4\pi)^3}$.

For a UAV with DFRC, the transmit power at each time slot includes communication power and radar detection power. Assuming that the total transmit power of the UAV at time slot q is $P_t(q)$, the power for communication and radar detection can be expressed as

$$P_{com}(q) = \alpha(q) P_t(q), \forall q \tag{14}$$

$$P_{rad}(q) = \Big(1 - \alpha(q)\Big) P_t(q), \forall q \tag{15}$$

where $0 \leq \alpha(q) \leq 1$ represents the power allocation factor in each time slot. Specifically, when the UAV performs the data upload task, $\alpha(q) = 1$.

B. System Performance Evaluation Metrics

To evaluate the performance of the UAV-assisted ISAC system, we present the following performance metrics. For the communication system, the information rate is defined as the average MI between the transmitter and the receiver, which is a crucial metric for measuring system performance. For the radar system, a novel metric based on information theory have been proposed, namely the radar estimation rate. If we consider the radar detection process as a scenario in which a target is unwilling to transmit its own information to the radar, we can describe the radar channel as a non-cooperative communication channel. In this case, the radar estimation rate can be defined as the MI between the radar and the target [16]. In order to measure the performance of the ISAC system using the same dimension, we have decided to use the information rate and radar estimation rate as the performance evaluation metrics of the ISAC system.

Due to the dual nature of the ISAC system, interference within the system must be taken into account. When communication and radar detection are carried out simultaneously, the communication receiver may experience interference from the radar signal, and the radar receiver may also be affected by the communication signal reflected by the radar target. Hence, when the UAV performs the ISAC task on the IoT node k, the signal to interference plus noise ratio (SINR) over

[3]To ensure the quality of sensing for the UAV, it is assumed that the UAV has a maximum detection angle and a maximum flight altitude, similar to the scheme described in references [38] and [39].

[4]According to experimental research on the UAV channel model in references [40] and [41], when the horizontal distance between the UAV and the IoT node is less than 1000m, and the UAV flight altitude is above 80m, it can be considered that the LoS link between the UAV and the IoT node is highly probable, approaching a probability of 1.

This is a peer-reviewed, accepted manuscript of the following paper: Liu, Z., Liu, X., Liu, Y., Leung, V. C. M., & Durrani, T. S. (2024). UAV assisted integrated sensing and communications for Internet of Things: 3D trajectory optimization and resource allocation. IEEE Transactions on Wireless Communications. Advance online publication. https://doi.org/10.1109/TWC.2024.3352985

communication channel and radar channel can be expressed as

$$\Gamma_{k,com}(q) = \frac{P_{com}(q)h_{k,com}(q)}{P_{rad}(q)h_{k,com}(q) + N_0 B}, \forall k, q \tag{16}$$

$$\Gamma_{k,rad}(q) = \frac{P_{rad}(q)h_{k,rad}(q)}{P_{com}(q)h_{k,rad}(q) + N_0 B}, \forall k, q \tag{17}$$

where B denotes the signal bandwidth, and N_0 represents the noise power spectral density.

According to the Shannon's theorem [36], the information rate from the UAV to the data collection center and node k at time slot q can be expressed as

$$R_c(q) = \log_2\left(1 + \frac{P_t(q)h_c(q)}{N_0 B}\right), \forall q \tag{18}$$

$$R_{k,com}(q) = \log_2\Big(1 + \Gamma_{k,com}(q)\Big), \forall k, q \tag{19}$$

Based on [24] and [37], the radar estimation rate of the UAV for the node k at time slot q can be described as

$$R_{k,rad}(q) = \log_2\Big(1 + \Gamma_{k,rad}(q)\Big), \forall k, q \tag{20}$$

To ensure that the nodes and data collection center can fully obtain the sensing information of the UAV, the amount of communication information transmitted to the nodes in each time slot should be no less than that of radar sensing information. Moreover, over the entire flight cycle, the amount of communication information transmitted to the data collection center should be no less than the total amount of radar sensing information for all the nodes. Hence, the communication constraints can be denoted as

$$R_{k,rad}(q) \le R_{k,com}(q), \forall k, q \tag{21}$$

$$\sum_{q=1}^{Q}\sum_{k=1}^{K}\omega_k(q)R_{k,rad}(q) \le \sum_{q=1}^{Q} b(q)R_c(q) \tag{22}$$

C. Problem Formulation

In the UAV assisted ISAC system, the main task of the UAV is to carry out the radar detection, and the purpose of communications is to transmit the radar sensing information to the data collection center and IoT nodes. Therefore, the information rate depends on the information capacity of the radar detection. Thus, in order to increase the amount of information detected by the radar, we seek to maximize the radar estimation rate by jointly optimizing UAV task scheduling $\mathbf{W} = \{\omega_k(q), b(q), \forall k, q\}$, UAV transmit power allocation $\mathbf{P} = \{P_t(q), \alpha(q), \forall q\}$ and UAV 3D flight parameters $\mathbf{L} = \{\mathbf{g}_u(q), \mathbf{v}(q), \forall q\}$. The optimization problem is given as

$$\max_{\mathbf{W},\mathbf{P},\mathbf{L}} \quad \sum_{q=1}^{Q}\sum_{k=1}^{K}\omega_k(q)R_{k,rad}(q) \tag{23a}$$

$$\text{s.t.} \quad \omega_k(q) \in \{0,1\}, \forall k, q \tag{23b}$$

$$b(q) \in \{0,1\}, \forall q \tag{23c}$$

$$\sum_{k=1}^{K}\omega_k(q) + b(q) = 1, \forall q \tag{23d}$$

$$\omega_k(q)\Big((x_u(q) - x_k)^2 + (y_u(q) - y_k)^2\Big) \le (H_u(q)\tan\theta)^2, \forall k, q \tag{23e}$$

$$R_{k,rad}(q) \le R_{k,com}(q), \forall k, q \tag{23f}$$

$$\sum_{q=1}^{Q}\sum_{k=1}^{K}\omega_k(q)R_{k,rad}(q) \le \sum_{q=1}^{Q} b(q)R_c(q) \tag{23g}$$

$$0 \le \frac{1}{Q}\sum_{q=1}^{Q} P_t(q) \le P_{avg} \tag{23h}$$

$$P_t(q) \ge 0, \forall q \tag{23i}$$

$$\mathbf{v}(1) = \mathbf{v}(Q) \tag{23j}$$

$$\mathbf{g}_u(1) = \mathbf{g}_u(Q) \tag{23k}$$

$$l_u(q+1) = l_u(q) + v_{xy}(q)\Delta t, \forall q \tag{23l}$$

$$H_u(q+1) = H_u(q) + v_z(q)\Delta t, \forall q \tag{23m}$$

$$\|v_{xy}(q+1) - v_{xy}(q)\| \le a_{xy}^{\max}, \forall q \tag{23n}$$

$$\|v_z(q+1) - v_z(q)\| \le a_z^{\max}, \forall q \tag{23o}$$

$$\|v_{xy}(q)\| \le v_{xy}^{\max}, \forall q \tag{23p}$$

$$\|v_z(q)\| \le v_z^{\max}, \forall q \tag{23q}$$

$$H_u^{\min} \le H_u(q) \le H_u^{\max}, \forall q \tag{23r}$$

where P_{avg} denotes the average transmit power of the UAV for each time slot, $v_{xy}^{\max}$ and $v_z^{\max}$ indicate the maximum horizontal and vertical velocities of the UAV, respectively; $H_u^{\min}$ and $H_u^{\max}$ represent the minimum and the maximum flight altitudes of the UAV, respectively.

III. Solution Algorithm

In this section, we illustrate the joint optimization framework for the UAV assisted ISAC system. Due to the integer vector $\mathbf{W}$ and the non-convex constraints (23e), (23f), (23g), we propose a three-layer iterative optimization algorithm to solve the mixed integer optimization problem (23), which divides the initial optimization problems into three parts: task scheduling optimization, sensing and communication power optimization, and 3D flight parameters optimization.

A. UAV Task Scheduling Optimization

To solve the integer vector $\mathbf{W}$, we first relax the binary variables $\omega_k(q)$ and $b(q)$ into continuous variables within the range of $[0, 1]$. Then, we loosen the strict equality constraint (23d), and replace it with an inequality constraint. Hence, the

This is a peer-reviewed, accepted manuscript of the following paper: Liu, Z., Liu, X., Liu, Y., Leung, V. C. M., & Durrani, T. S. (2024). UAV assisted integrated sensing and communications for Internet of Things: 3D trajectory optimization and resource allocation. IEEE Transactions on Wireless Communications. Advance online publication. https://doi.org/10.1109/TWC.2024.3352985

task scheduling optimization problem with the fixed power allocation $\mathbf{P}$ and flight parameters $\mathbf{L}$ can be formulated as

$$\max_{\mathbf{W}} \quad \sum_{q=1}^{Q}\sum_{k=1}^{K}\omega_k(q)R_{k,rad}(q) \tag{24a}$$

$$\text{s.t.} \quad 0 \le \omega_k(q) \le 1, \forall k, q \tag{24b}$$

$$0 \le b(q) \le 1, \forall q \tag{24c}$$

$$\sum_{k=1}^{K}\omega_k(q) + b(q) \le 1, \forall q \tag{24d}$$

$$\omega_k(q)\Big((x_u(q)-x_k)^2 + (y_u(q)-y_k)^2\Big) \le (H_u(q)\tan\theta)^2, \forall k, q \tag{24e}$$

$$\sum_{q=1}^{Q}\sum_{k=1}^{K}\omega_k(q)R_{k,rad}(q) \le \sum_{q=1}^{Q}b(q)R_c(q) \tag{24f}$$

which is a convex optimization problem that can be solved by the Matlab CVX directly.

Then, the continuous variables $\omega_k(q)$ and $b(q)$ obtained by the CVX need to be converted back to their original discrete binary form. If the difference between $\omega_k(q)$, $b(q)$ and 1 is less than the maximum tolerance δ, then $\omega_k(q)$ and $b(q)$ will be set to 1. Otherwise, they will be set to 0. After obtaining the binary solutions of $\omega_k(q)$ and $b(q)$, we can achieve the complete binary integer solution of $\mathbf{W}$.

B. UAV Sensing and communication Power Optimization

With the fixed UAV task scheduling $\mathbf{W}$ and UAV flight parameters $\mathbf{L}$, the UAV transmit power allocation problem is given as

$$\max_{\mathbf{P}} \quad \sum_{q=1}^{Q}\sum_{k=1}^{K}\omega_k(q)R_{k,rad}(q) \tag{25a}$$

$$\text{s.t.} \quad R_{k,rad}(q) \le R_{k,com}(q), \forall k, q \tag{25b}$$

$$\sum_{q=1}^{Q}\sum_{k=1}^{K}\omega_k(q)R_{k,rad}(q) \le \sum_{q=1}^{Q}b(q)R_c(q) \tag{25c}$$

$$0 \le \frac{1}{Q}\sum_{q=1}^{Q}P_t(q) \le P_{avg} \tag{25d}$$

$$P_t(q) \ge 0, \forall q \tag{25e}$$

$$0 \le \alpha(q) \le 1, \forall q \tag{25f}$$

which is a non-convex optimization problem with no closed-form solutions for $\alpha(q)$ and $P_t(q)$. Therefore, we use the SCA method to solve it.

Since the objective function contains two variables $\alpha(q)$ and $P_t(q)$, the problem (25) is difficult to solve directly. Therefore, (25) is divided into two sub-problems as

$$\max_{\mathbf{A}} \quad \sum_{q=1}^{Q}\sum_{k=1}^{K}\omega_k(q)R_{k,rad}(q) \tag{26a}$$

$$\text{s.t.} \quad (25b), (25c), (25f) \tag{26b}$$

$$\max_{\hat{\mathbf{P}}} \quad \sum_{q=1}^{Q}\sum_{k=1}^{K}\omega_k(q)R_{k,rad}(q) \tag{27a}$$

$$\text{s.t.} \quad (25b) \sim (25e) \tag{27b}$$

where $\mathbf{A} = \{\alpha(q), \forall q\}$ and $\hat{\mathbf{P}} = \{P_t(q), \forall q\}$ represent the power allocation factor and transmit power of the UAV, respectively.

With the SCA algorithm, we first convert the non-linear problems (26) and (27) into linear problems. For any local points $\alpha^{(i)}(q)$ and $P_t^{(i)}(q)$, $R_{k,rad}(q)$ and $R_{k,com}(q)$ in (26) and (27) can be replaced by their first-order Taylor expansions, which can be written as

$$R_{k,rad}^{\alpha}(q) = \log_2\left(1+\frac{(1-\alpha^{(i)}(q))P_t(q)h_{k,rad}(q)}{\alpha^{(i)}(q)P_t(q)h_{k,rad}(q)+N_0B}\right) - \frac{P_t(q)h_{k,rad}(q)}{\ln 2(N_0B+\alpha^{(i)}(q)P_t(q)h_{k,rad}(q))}\left(\alpha(q)-\alpha^{(i)}(q)\right) \tag{28}$$

$$R_{k,com}^{\alpha}(q) = \log_2\left(1+\frac{\alpha^{(i)}(q)P_t(q)h_{k,com}(q)}{(1-\alpha^{(i)}(q))P_t(q)h_{k,com}(q)+N_0B}\right) + \frac{P_t(q)h_{k,com}(q)}{\ln 2(N_0B+(1-\alpha^{(i)}(q))P_t(q)h_{k,rad}(q))}\left(\alpha(q)-\alpha^{(i)}(q)\right) \tag{29}$$

$$R_{k,rad}^{p}(q) = \log_2\left(1+\frac{(1-\alpha(q))P_t^{(i)}(q)h_{k,rad}(q)}{\alpha(q)P_t^{(i)}(q)h_{k,rad}(q)+N_0B}\right) + \psi_{p,rad}\left(P_t(q)-P_t^{(i)}(q)\right) \tag{30}$$

$$R_{k,com}^{p}(q) = \log_2\left(1+\frac{\alpha(q)P_t^{(i)}(q)h_{k,com}(q)}{(1-\alpha(q))P_t^{(i)}(q)h_{k,com}(q)+N_0B}\right) + \psi_{p,com}\left(P_t(q)-P_t^{(i)}(q)\right) \tag{31}$$

where,

$$\psi_{p,rad} = \frac{h_{k,rad}(q)}{\ln 2(N_0B+P_t^{(i)}(q)h_{k,rad}(q))} - \frac{\alpha(q)h_{k,rad}(q)}{\ln 2(N_0B+\alpha(q)P_t^{(i)}(q)h_{k,rad}(q))} \tag{32}$$

$$\psi_{p,com} = \frac{h_{k,com}(q)}{\ln 2(N_0B+P_t^{(i)}(q)h_{k,com}(q))} - \frac{(1-\alpha(q))h_{k,com}(q)}{\ln 2(N_0B+(1-\alpha(q))P_t^{(i)}(q)h_{k,com}(q))} \tag{33}$$

Then, problems (26) and (27) can be redescribed as

$$\max_{\mathbf{A}} \quad \sum_{q=1}^{Q}\sum_{k=1}^{K}\omega_k(q)R_{k,rad}^{\alpha}(q) \tag{34a}$$

$$\text{s.t.} \quad R_{k,rad}^{\alpha}(q) \le R_{k,com}^{\alpha}(q), \forall k, q \tag{34b}$$

$$\sum_{q=1}^{Q}\sum_{k=1}^{K}\omega_k(q)R_{k,rad}^{\alpha}(q) \le \sum_{q=1}^{Q}b(q)R_c(q) \tag{34c}$$

$$0 \le \alpha(q) \le 1, \forall q \tag{34d}$$

This is a peer-reviewed, accepted manuscript of the following paper: Liu, Z., Liu, X., Liu, Y., Leung, V. C. M., & Durrani, T. S. (2024). UAV assisted integrated sensing and communications for Internet of Things: 3D trajectory optimization and resource allocation. IEEE Transactions on Wireless Communications. Advance online publication. https://doi.org/10.1109/TWC.2024.3352985

$$\max_{\hat{\mathbf{P}}} \quad \sum_{q=1}^{Q}\sum_{k=1}^{K}\omega_k(q)R_{k,rad}^{p}(q) \tag{35a}$$

$$\text{s.t.} \quad R_{k,rad}^{p}(q) \le R_{k,com}^{p}(q), \forall k, q \tag{35b}$$

$$\sum_{q=1}^{Q}\sum_{k=1}^{K}\omega_k(q)R_{k,rad}^{p}(q) \le \sum_{q=1}^{Q} b(q)R_c(q) \tag{35c}$$

$$0 \le \frac{1}{Q}\sum_{q=1}^{Q} P_t(q) \le P_{avg} \tag{35d}$$

$$P_t(q) \ge 0, \forall q \tag{35e}$$

Obviously, (34) and (35) are convex and can be solved by the CVX, respectively. However, the obtained solutions for $\alpha(q)$ and $P_t(q)$ at this time are not the optimal solutions of problem (25). Therefore, we need to approximate the optimal solution of (25) through iterative optimization. The specific iterative process is shown in Algorithm 1.

Algorithm 1 Transmit power allocation optimization.

Initialize: the power allocation factor $\mathbf{A}^{(i)}$, the UAV transmit power $\hat{\mathbf{P}}^{(i)}$, and the maximum tolerance δ;

1: **repeat**
2: fixing $\hat{\mathbf{P}}^{(i)}$, solve (34) to get solution $\mathbf{A}^{(i+1)}$;
3: fixing $\mathbf{A}^{(i+1)}$, solve (35) to get solution $\hat{\mathbf{P}}^{(i+1)}$;
4: set $i = i + 1$;
5: **until** the growth of target value is less than δ;

Output: UAV transmit power allocation $\mathbf{P} = \{\hat{\mathbf{P}}, \mathbf{A}\}$

C. UAV 3D Flight Parameters Optimization

With the fixed UAV task scheduling $\mathbf{W}$ and UAV transmit power allocation $\mathbf{P}$, the UAV 3D flight parameters optimization problem is given as

$$\max_{\mathbf{L}} \quad \sum_{q=1}^{Q}\sum_{k=1}^{K}\omega_k(q)R_{k,rad}(q) \tag{36a}$$

$$\text{s.t.} \quad \omega_k(q)\Big((x_u(q)-x_k)^2 + (y_u(q)-y_k)^2\Big) \le (H_u(q)\tan\theta)^2, \forall k, q \tag{36b}$$

$$R_{k,rad}(q) \le R_{k,com}(q), \forall k, q \tag{36c}$$

$$\sum_{q=1}^{Q}\sum_{k=1}^{K}\omega_k(q)R_{k,rad}(q) \le \sum_{q=1}^{Q} b(q)R_c(q) \tag{36d}$$

$$l_u(q+1) = l_u(q) + v_{xy}(q)\Delta t, \forall q \tag{36e}$$

$$H_u(q+1) = H_u(q) + v_z(q)\Delta t, \forall q \tag{36f}$$

$$\|v_{xy}(q+1) - v_{xy}(q)\| \le a_{xy}^{\max}, \forall q \tag{36g}$$

$$\|v_z(q+1) - v_z(q)\| \le a_z^{\max}, \forall q \tag{36h}$$

$$\|v_{xy}(q)\| \le v_{xy}^{\max}, \forall q \tag{36i}$$

$$\|v_z(q)\| \le v_z^{\max}, \forall q \tag{36j}$$

$$\mathbf{v}(1) = \mathbf{v}(Q) \tag{36k}$$

$$\mathbf{g}_u(1) = \mathbf{g}_u(Q) \tag{36l}$$

$$H_u^{\min} \le H_u(q) \le H_u^{\max}, \forall q \tag{36m}$$

Since the objective function (36a) and constraint (36b) $\sim$ (36d) are all non-convex, we need to convert them into linear convex functions, so that (36) can be solved by the CVX.

For the constraint (36b), we replace the square term on the right side of the inequality with a first-order linear function at the local point $H_u^{(i)}(q)$, which can be denoted as

$$(H_u(q)tan\theta)^2 \ge H_u^{lf}(q) = (H_u^{(i)}(q)tan\theta)^2 + 2tan^2\theta H_u^{(i)}(q)\Big(H_u(q) - H_u^{(i)}(q)\Big) \tag{37}$$

For the objective function (36a) and constraints (36c), (36d), by substituting (11), (12) and (13) into $R_c(q)$, $R_{k,com}(q)$ and $R_{k,rad}(q)$, respectively, we can get the data upload rate, communication rate and radar estimation rate with d_c^2 and d_k^2 as

$$R_c(q) = \log_2\left(1 + \frac{P_t(q)\beta_{com}}{N_0 B d_c^2}\right) \tag{38}$$

$$R_{k,com}(q) = \log_2\left(1 + \frac{P_{com}(q)\beta_{com}}{P_{rad}(q)\beta_{com} + N_0 B d_k^2}\right) \tag{39}$$

$$R_{k,rad}(q) = \log_2\left(1 + \frac{P_{rad}(q)\beta_{rad}}{P_{com}(q)\beta_{rad} + N_0 B d_k^4}\right) \tag{40}$$

To convert the above expression, we introduce the following lemma.

Lemma 1: If A_1, B_1, C_1 are positive, the lower bound of the function $\log_2(1 + \frac{A_1}{B_1 + C_1 X})$ at the local point $X^{(i)}$ can be written as

$$\log_2(1 + \frac{A_1}{B_1 + C_1 X}) \ge \log_2(1 + \frac{A_1}{B_1 + C_1 X^{(i)}}) - \frac{A_1 C_1 (X - X^{(i)})}{\ln 2 (B_1 + C_1 X)(A_1 + B_1 + C_1 X)} \tag{41}$$

Proof: Please refer to Appendix A. ∎

According to Lemma 1, for the fixed points $\| \mathbf{g}_u^{(i)}(q) - \mathbf{g}_c\|^2$ and $\| \mathbf{g}_u^{(i)}(q) - \mathbf{g}_k\|^2$, the first order Taylor expansion is used to replace R_c and $R_{k,com}$ with their lower bounds and to replace $R_{k,rad}$ with its linear form, which are described as

$$R_c(q) \ge R_c^{lf}(q) = R_c^{(i)}(q) + \xi_c^{(i)} D_c^{(i)}(q), \forall q \tag{42}$$

$$R_{k,com}(q) \ge R_{k,com}^{lf}(q) = R_{k,com}^{(i)}(q) - \xi_{k,com}^{(i)} D_k^{(i)}(q), \forall k, q \tag{43}$$

$$R_{k,rad}(q) = R_{k,rad}^{lf}(q) = R_{k,rad}^{(i)}(q) - \xi_{k,rad}^{(i)} D_k^{(i)}(q), \forall k, q \tag{44}$$

where $R_{k,com}^{(i)}(q)$, $R_{k,rad}^{(i)}(q)$, $\xi_c^{(i)}$, $\xi_{k,com}^{(i)}$ and $\xi_{k,rad}^{(i)}$ are given in (45) $\sim$ (49) at the top of the next page, $R_c^{(i)}(q)$, $D_c^{(i)}(q)$ and $D_k^{(i)}(q)$ are respectively given as

$$R_c^{(i)}(q) = \log_2\left(1 + \frac{P_t(q)\beta_{com}}{N_0 B \left\| \mathbf{g}_u^{(i)}(q) - \mathbf{g}_c \right\|^2}\right), \forall q \tag{50}$$

This is a peer-reviewed, accepted manuscript of the following paper: Liu, Z., Liu, X., Liu, Y., Leung, V. C. M., & Durrani, T. S. (2024). UAV assisted integrated sensing and communications for Internet of Things: 3D trajectory optimization and resource allocation. IEEE Transactions on Wireless Communications. Advance online publication. https://doi.org/10.1109/TWC.2024.3352985

$$R_{k,com}^{(i)}(q)=\log_2\left(1+\frac{P_{com}(q)\beta_{com}}{P_{rad}(q)\beta_{com}+N_0B\left\|\mathbf{g}_u^{(i)}(q)-\mathbf{g}_k\right\|^4}\right),\forall k,q \tag{45}$$

$$R_{k,rad}^{(i)}(q)=\log_2\left(1+\frac{P_{rad}(q)\beta_{rad}}{P_{com}(q)\beta_{rad}+N_0B\left\|\mathbf{g}_u^{(i)}(q)-\mathbf{g}_k\right\|^4}\right),\forall k,q \tag{46}$$

$$\xi_c^{(i)}=-\frac{\beta_{com}P_t(q)}{\ln 2\left(N_0B\left\|\mathbf{g}_u^{(i)}(q)-\mathbf{g}_k\right\|^4+\beta_{com}P_t(q)\left\|\mathbf{g}_u^{(i)}(q)-\mathbf{g}_k\right\|^2\right)},\forall q \tag{47}$$

$$\xi_{k,com}^{(i)}=\frac{N_0B\alpha(q)P_t\left(q\right)\beta_{com}}{\ln 2(((1-\alpha)P_t\left(q\right)\beta_{com}+N_0B\parallel\mathbf{g}_u(q)-\mathbf{g}_k\parallel^2)^2+\alpha P_t\left(q\right)\beta_{com}((1-\alpha)P_t\left(q\right)\beta_{com}+N_0B\parallel\mathbf{g}_u(q)-\mathbf{g}_k\parallel^2))} \tag{48}$$

$$\xi_{k,rad}^{(i)}=\frac{2N_0B(1-\alpha(q))P_t\left(q\right)\beta_{rad}\parallel\mathbf{g}_u^{(i)}(q)-\mathbf{g}_k\parallel^2}{\ln 2((\alpha(q)P_t\left(q\right)\beta_{rad}+N_0B\parallel\mathbf{g}_u^{(i)}(q)-\mathbf{g}_k\parallel^4)^2+(1-\alpha(q))P_t\left(q\right)\beta_{rad}(\alpha(q)P_t\left(q\right)\beta_{rad}+N_0B\parallel\mathbf{g}_u^{(i)}(q)-\mathbf{g}_k\parallel^4))} \tag{49}$$

$$D_c^{(i)}(q)=\parallel\mathbf{g}_u(q)-\mathbf{g}_c\parallel^2-\parallel\mathbf{g}_u^{(i)}(q)-\mathbf{g}_c\parallel^2,\forall q \tag{51}$$

$$D_k^{(i)}(q)=\parallel\mathbf{g}_u(q)-\mathbf{g}_k\parallel^2-\parallel\mathbf{g}_u^{(i)}(q)-\mathbf{g}_k\parallel^2,\forall k,q \tag{52}$$

After obtaining the substitution functions of $R_c(q)$, $R_{k,com}(q)$ and $R_{k,rad}(q)$, due to the existence of the square terms $D_c^{(i)}(q)$ and $D_k^{(i)}(q)$, (36c) and (36d) still do not comply with the usage rules of the CVX. Hence, we introduce two auxiliary variables $\kappa(q)$ and $\tau_k(q)$ to relax the functions $R_c^{lf}(q)$, $R_{k,com}^{lf}(q)$ and $R_{k,rad}^{lf}(q)$, which can be written as

$$\kappa(q)\geq D_c^{(i)}(q),\forall q \tag{53}$$

$$\tau_k(q)\geq D_k^{(i)}(q),\forall q \tag{54}$$

$$R_c^{lf}(q)\geq R_c^s(q)=R_c^{(i)}(q)+\xi_c^{(i)}\kappa(q),\forall q \tag{55}$$

$$R_{k,com}^{lf}(q)\geq R_{k,com}^s(q)=R_{k,com}^{(i)}(q)-\xi_{k,com}^{(i)}\tau_k(q),\forall k,q \tag{56}$$

$$R_{k,rad}^{lf}(q)\geq R_{k,rad}^s(q)=R_{k,rad}^{(i)}(q)-\xi_{k,rad}^{(i)}\tau_k(q),\forall k,q \tag{57}$$

Therefore, the optimization problem (36) for UAV flight parameters $\mathbf{L}$ can be redescribed as

$$\max_{\mathbf{L}}\quad\sum_{q=1}^{Q}\sum_{k=1}^{K}\omega_k(q)R_{k,rad}^s(q) \tag{58a}$$

$$\text{s.t.}\quad\omega_k(q)\left((x_u(q)-x_k)^2+(y_u(q)-y_k)^2\right)\leq H_u^{lf}(q) \tag{58b}$$

$$R_{k,rad}^s(q)\leq R_{k,com}^s(q),\forall k,q \tag{58c}$$

$$\sum_{q=1}^{Q}\sum_{k=1}^{K}\omega_k(q)R_{k,rad}^s(q)\leq\sum_{q=1}^{Q}b(q)R_c^s(q) \tag{58d}$$

$$(36e)\sim(36m) \tag{58e}$$

which is convex and can be solved by continuously updating the values of $R_{k,rad}^s(q)$, $R_{k,com}^s(q)$ and $R_c^s(q)$ through the CVX.

D. Three Layer Iterative Optimization

By solving problems (24), (25) and (58), we obtain the optimal solutions of $\mathbf{W}$, $\mathbf{P}$ and $\mathbf{L}$ to the three subproblems, respectively. To get the optimal solutions to the original problem (23), we propose a three-layer iterative optimization algorithm to iteratively optimize the three subproblems until the objective function value is convergent, as shown in Algorithm 2.

Lemma 2: Algorithm 2 is convergent.

Proof: Please refer to Appendix B. ■

Algorithm 2 Three-layer iterative optimization.

Initialize: the maximum tolerance δ, the UAV task scheduling $\mathbf{W}^{(i)}$, the UAV transmit power allocation $\mathbf{P}^{(i)}$, the UAV flight parameters $\mathbf{L}^{(i)}$ and the value of objective function $R_{rad}^{(i)}$;

1: **while** $|R_{rad}^{(i)}-R_{rad}^{(i-1)}|>\delta$ **do**
2: fixing $\mathbf{P}^{(i)}$ and $\mathbf{L}^{(i)}$, solve (24) to get solution $\mathbf{W}^{(i+1)}$;
3: fixing $\mathbf{W}^{(i+1)}$ and $\mathbf{L}^{(i)}$, solve (25) to get solution $\mathbf{P}^{(i+1)}$;
4: fixing $\mathbf{W}^{(i+1)}$ and $\mathbf{P}^{(i+1)}$, solve (58) to get solution $\mathbf{L}^{(i+1)}$;
5: set $i=i+1$;
6: **end while**

Output: $\mathbf{W}$, $\mathbf{P}$, $\mathbf{L}$.

IV. Simulation Results

In this section, we conduct simulation experiments to demonstrate the rationality of the system model and the validity of the optimization scheme. According to [10], [18], [24] and [25], the values of parameters used in the simulation experiments are shown in Table II. We assume a square area of 1200m × 1200m, where 12 IoT nodes are randomly distributed and the data collection center is located at the center of the area. To get the optimal UAV 3D trajectory, we first define an initial flight trajectory of the UAV, which is a circle with the data collection center as the center and the radius of

This is a peer-reviewed, accepted manuscript of the following paper: Liu, Z., Liu, X., Liu, Y., Leung, V. C. M., & Durrani, T. S. (2024). UAV assisted integrated sensing and communications for Internet of Things: 3D trajectory optimization and resource allocation. IEEE Transactions on Wireless Communications. Advance online publication. https://doi.org/10.1109/TWC.2024.3352985

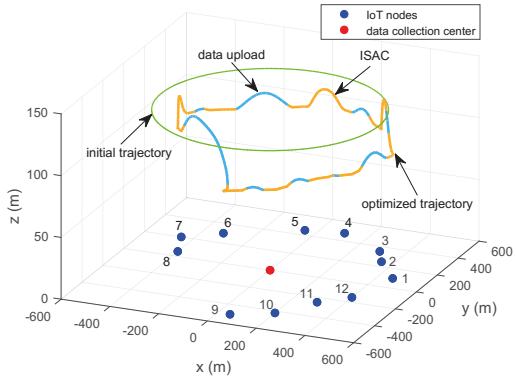

(a) Optimized 3D trajectory and task scheduling of the UAV.

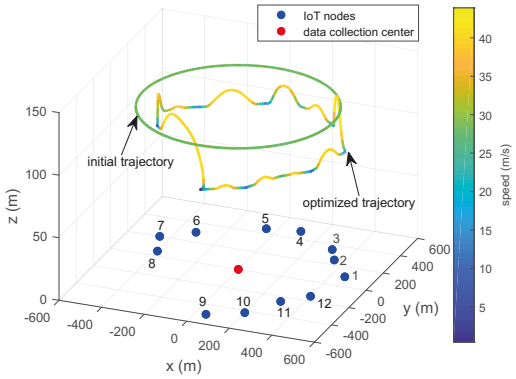

(b) Optimized 3D trajectory and flight speed of the UAV.

Fig. 2. Initial and optimized 3D UAV trajectory.

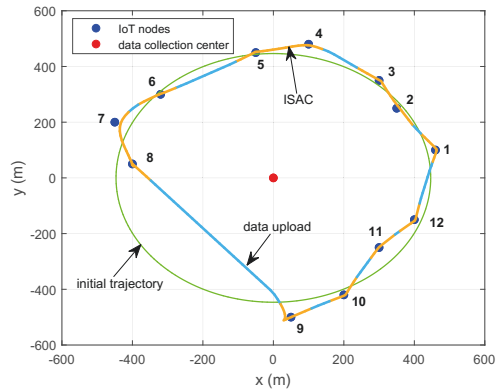

(a) Top view of optimized 3D UAV trajectory and task scheduling.

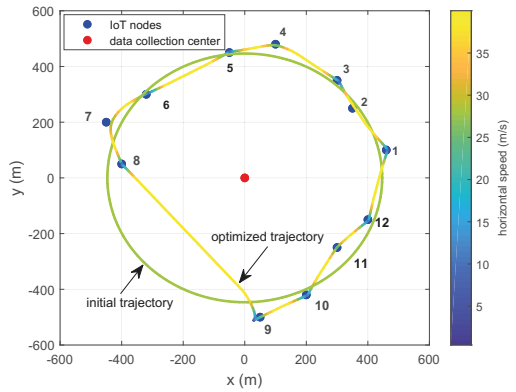

(b) Top view of optimized 3D UAV trajectory and horizontal speed.

Fig. 3. Top view of the initial and optimized 3D UAV trajectory.

TABLE II
SIMULATION PARAMETERS

Parameter	Value
number of IoT nodes	$K = 12$
total flight time of the UAV	$T = 100$ s
time interval	$\Delta t = 0.5$ s
maximum horizontal speed of the UAV	$v_{xy}^{\max} = 40$ m/s
maximum vertical speed of the UAV	$v_{z}^{\max} = 20$ m/s
maximum horizontal acceleration of the UAV	$a_{xy}^{\max} = 5$ m/s^2
maximum vertical acceleration of the UAV	$a_{z}^{\max} = 5$ m/s^2
maximum detection angle of the UAV	$\theta = 30°$
minimum flight altitude of the UAV	$H_u^{\min} = 100$ m
maximum flight altitude of the UAV	$H_u^{\max} = 200$ m
average transmit power of the UAV	$P_{avg} = 1$ W
carrier frequency	$f_c = 3.5$ GHz
bandwidth	$B = 50$ MHz
noise power spectral density	$N_0 = -160$ dBmW/Hz
RCS of the target	$\sigma = 1$ m^2
antenna gain of the UAV transmitter	$G_t = 17$ dBi
antenna gain of the UAV receiver	$G_r = 17$ dBi
communication receiver antenna gain	$G_c = 0$ dBi
maximum tolerance	$\delta = 10^{-4}$

$r = \frac{\max\|l_c - l_k\| + \min\|l_c - l_k\|}{2}$. The UAV flies over the target area at constant altitude $H_{init} = \frac{H_u^{\max} + H_u^{\min}}{2}$ and speed in the initial trajectory. Therefore, the initial velocity and trajectory of the UAV can be denoted by

$$\mathbf{v}_{init}(q) = \left(\frac{2\pi r}{T}\cos\gamma, \frac{2\pi r}{T}\sin\gamma, 0\right), \forall q \tag{59}$$

$$\mathbf{g}_u^{init}(q) = \left(r\cos\gamma, r\sin\gamma, H_{init}\right), \forall q \tag{60}$$

where,

$$\gamma = \frac{2\pi(q-1)}{Q-1} + \arcsin\frac{y_1}{\|l_1 - l_c\|} \tag{61}$$

Furthermore, based on the initial 3D flight parameters, we set the initial UAV transmit power $P_t(q)$=1W and the initial power allocation factor $\alpha(q)$=0.5.

Under the above initial conditions, we first present the optimized 3D trajectory obtained by Algorithm 2 in Fig. 2. The numbers next to the nodes denote the node indexes. In Fig. 2(a), the orange line segment represents the flight trajectory of the UAV when performing the ISAC task, while the blue line segment represents the flight trajectory of the UAV when performing the data upload task. It can be observed that the UAV frequently changes its flight altitude to better perform ISAC and data upload task. When the radar sensing angle θ is fixed, a higher flight altitude means a larger ground detection

This is a peer-reviewed, accepted manuscript of the following paper: Liu, Z., Liu, X., Liu, Y., Leung, V. C. M., & Durrani, T. S. (2024). UAV assisted integrated sensing and communications for Internet of Things: 3D trajectory optimization and resource allocation. IEEE Transactions on Wireless Communications. Advance online publication. https://doi.org/10.1109/TWC.2024.3352985

range. Therefore, when some nodes are close (nodes 7 and 8, nodes 4 and 5, nodes 2 and 3), to maximize the radar estimation rate, the UAV will fly to a higher altitude to sense more nodes. Meanwhile, to obtain the better radar channel gain, the UAV will perform the ISAC task at a lower altitude when sensing only one node. In Fig. 2(b), different colors represent different flight speeds, and the lighter the color, the higher the flight speed, as shown in the colorbar at the right. It can be seen that the UAV will fly slower when performing the ISAC task, which will achieve longer sensing time to improve the radar estimation information.

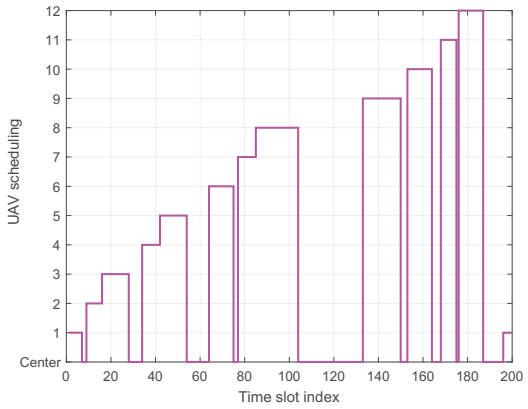

Fig. 4. Task scheduling of the UAV.

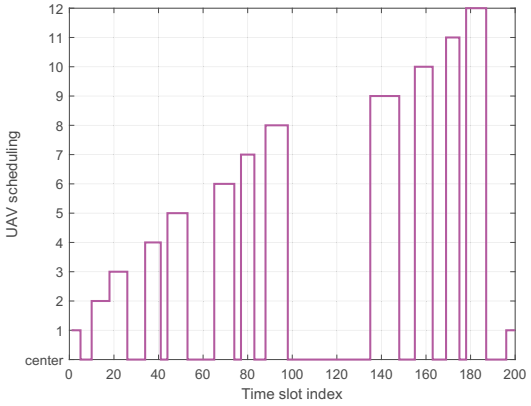

Fig. 5. Task scheduling of the UAV at the constant flight altitude 100m.

In order to show the status of the UAV more clearly, we plot the top view of the optimized 3D trajectory in Fig. 3. We can observe that the UAV will fly above the nodes as much as possible to execute the ISAC task, so as to obtain better channel condition and more detection information. Furthermore, the UAV mostly flies directly between the nodes at a high speed, which will reduce the flight time and allow more time for the ISAC task.

Figure 4 depicts the scheduling of UAV tasks in each time slot. The y-axis represents the index of the nodes and data collection center. When the UAV performs a task on a specific target, the y-axis value is set to the corresponding node index. It can be observed that the UAV performs the ISAC task on each node and uploads the detected information to the data collection center within the detection interval. Moreover, when flying over nodes with relatively short distances, such as nodes 4 and 5 or nodes 7 and 8, the UAV increases its flight altitude and performs the ISAC task for a longer duration to sense more nodes and obtain more detection information. This is significantly different from the results in Fig. 5, which do not optimize the flight altitude.

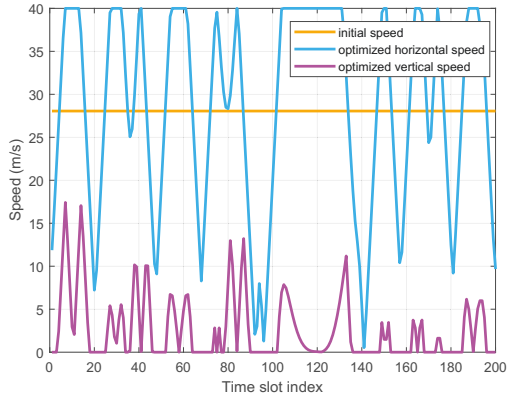

Fig. 6. Initial and optimized speeds of the UAV.

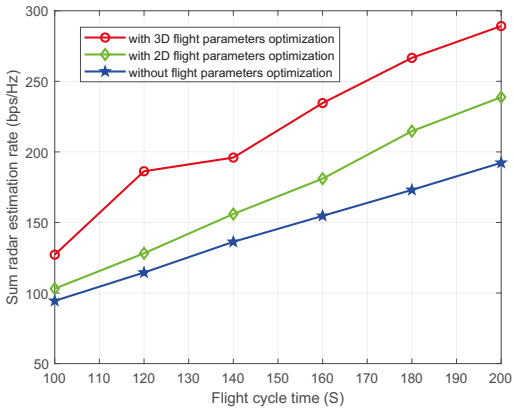

Fig. 7. The radar estimation rate for different optimization schemes versus the flight cycle time.

Figure 6 shows the initial and optimized speeds of the UAV. We can see that unlike the uniform UAV speed in the initial trajectory, the optimized UAV speed exhibits large fluctuations. By comparing the task scheduling of the UAV in Fig. 4, we can observe that in the horizontal direction, the UAV always flies at a lower speed when performing the ISAC task but at full speed when performing the data upload task. Similarly, in the vertical direction, the UAV hardly changes its speed when executing the ISAC task. This is because the UAV decreases its flight speed when flying over the nodes to stay around the nodes longer and obtain more detection information. To further illustrate the improvement of the system performance by optimizing the 3D flight parameters, we make some comparisons in Fig. 7.

Figure 7 shows a comparison of the sum radar estimation

This is a peer-reviewed, accepted manuscript of the following paper: Liu, Z., Liu, X., Liu, Y., Leung, V. C. M., & Durrani, T. S. (2024). UAV assisted integrated sensing and communications for Internet of Things: 3D trajectory optimization and resource allocation. IEEE Transactions on Wireless Communications. Advance online publication. https://doi.org/10.1109/TWC.2024.3352985

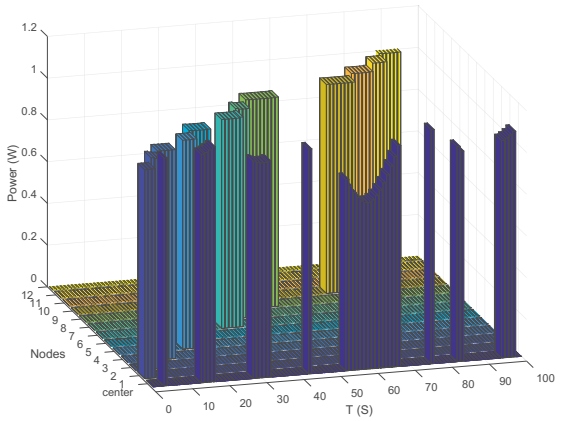

Fig. 8. The optimized transmit power for data collection center and nodes.

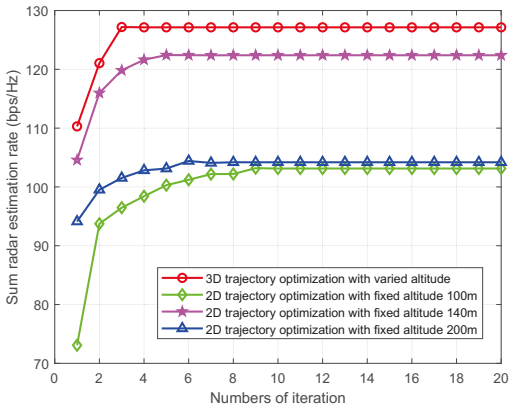

Fig. 10. The radar estimation rate for different flight altitude versus the number of iterations.

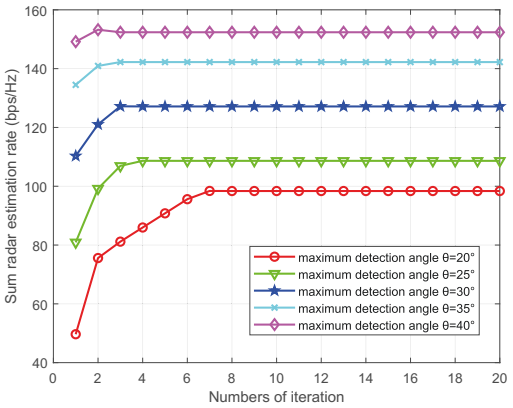

Fig. 9. The radar estimation rate for different maximum detection angle versus the number of iterations.

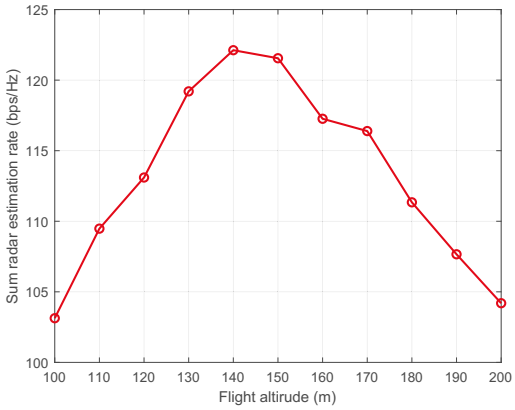

Fig. 11. The radar estimation rate for different flight altitude.

rate between different optimization schemes. The red line represents the sum radar estimation rate obtained by jointly optimizing the 3D flight trajectory and velocity, with maximum horizontal and vertical speeds set to 40 $\mathrm{m/s}$ and 20 $\mathrm{m/s}$, respectively. The green line shows the result of optimizing only the 2D trajectory, with a maximum horizontal speed of $\|\mathbf{v}_{xy}(q)\| = 40$ $\mathrm{m/s}$, while the blue line shows the result without optimizing any flight parameters. It can be observed that optimizing the 3D flight trajectory results in a higher sum radar estimation rate compared to the other two schemes.

Figure 8 shows the transmit power allocated by the UAV to the mission target in each time slot. It can be seen that the UAV will use less time and power for data upload tasks to ensure sensing performance, because the communication channel gain is better than the sensing channel gain due to the signal attenuation caused by the radar sensing echo.

Figure 9 compares the convergence of Algorithm 2 for different maximum detection angles θ. We can see that increasing the maximum detection angle of the UAV can effectively improve the sum radar detection rate. This is because the coverage of the UAV radar gradually becomes larger as the maximum detection angle increases, allowing the UAV more time to perform the ISAC task. Furthermore, we observe that the convergence speed of Algorithm 2 imporves gradually with the increase of the maximum detection angle. This is because when the detection range of the UAV radar is small, the UAV flight trajectory has greater uncertainty, and thus more iterations are needed to obtain a stable trajectory.

Figure 10 compares the sum radar estimation rates between 3D flight parameters optimization with varied altitude and 2D flight parameters optimization with fixed altitudes. In the case of the fixed altitude, we can see that the sum radar estimation rate does not always increase with the rise of the flight altitude. To illustrate the effect of different fixed flight altitude on the system performance, we show the sum radar estimation rate versus the flight altitude in Figure 11. It can be observed that as the flight altitude rises, the sum radar estimation rate first increases to the maximum value at an altitude of 140m and then decreases. This is because when the flight altitude initially rises, the UAV will have a larger detection range on the ground nodes, thereby obtaining more detection information. However, when the flight altitude exceeds a certain level, the channel condition between the UAV and the node will deteriorate, offsetting the positive gain from the greater detection range, which ultimately results in degraded system performance. However, as shown in Figure 10, the maximum sum radar estimation rate of the 2D flight

This is a peer-reviewed, accepted manuscript of the following paper: Liu, Z., Liu, X., Liu, Y., Leung, V. C. M., & Durrani, T. S. (2024). UAV assisted integrated sensing and communications for Internet of Things: 3D trajectory optimization and resource allocation. IEEE Transactions on Wireless Communications. Advance online publication. https://doi.org/10.1109/TWC.2024.3352985

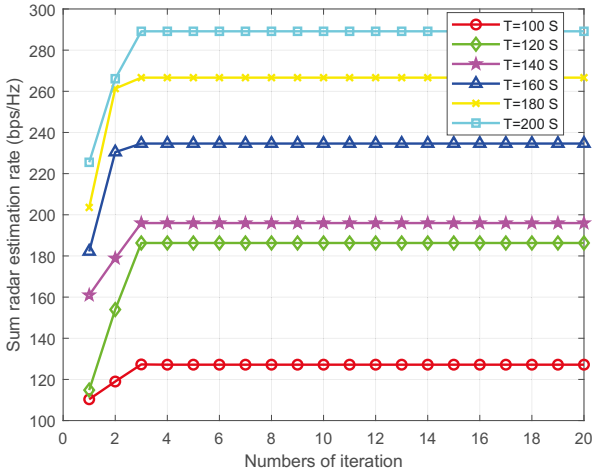

Fig. 12. The radar estimation rate for different flight cycle time versus the number of iterations.

parameters optimization with the altitude of 140m is still less than that of the 3D flight parameters optimization with varied altitude.

Figuer 12 compares the convergence of Algorithm 2 for different flight cycle time T. We can see that increasing the flight cycle time can significantly improve the system performance. This is because as the flight time increases, the UAV has more time to perform the ISAC task, which leads to an increase in the sum radar estimation rate.

V. Conclusions

In this paper, we propose a UAV-assisted ISAC model for IoT, where a UAV is dispatched as an aerial service platform to provide ISAC and data upload services for ground nodes and the data collection center. To evaluate the sensing performance of the ISAC system, we introduce the radar estimation rate as an important metric, which is maximized by formulating a mixed-integer programming problem. The non-convex mixed-integer optimization problem is divided into three subproblems, and the optimal solutions can be obtained by proposing a three-layer iterative optimization algorithm to iteratively optimize the three subproblems. From the simulation results, we draw the following conclusions. Firstly, the radar estimation rate effectively indicates the sensing performance of the ISAC system. Secondly, optimizing the 3D flight parameters can significantly improve the radar detection performance of the ISAC system. Finally, the impact of flight altitude on system performance is not monotonous, and optimizing the flight altitude can better leverage the advantages of UAV-assisted ISAC. Additionally, the future work could consider the situations of ground node motion and multi-UAV-assisted ISAC.

Appendix A
Proof of Lemma 1

Define the function $f(X) = \log_2(1+\frac{A_1}{B_1+C_1X})$ with $X > 0$ and $A_1, B_1, C_1 > 0$. Then, the first-order and second-order derivatives of $f(X)$ can be written as

$$f'(X) = -\frac{A_1C_1}{\ln 2(B_1+C_1X)(A_1+B_1+C_1X)} \tag{62}$$

$$f''(X) = \frac{A_1C_1^2(2C_1X+2B_1C_1+A_1)}{\ln 2\big((B_1+C_1X)^2+A_1C_1X+A_1B_1\big)^2} \tag{63}$$

Since X, A_1, B_1, C_1 are positive, we can get $f''(X) > 0$, which means that $f(X)$ is a convex function with respect to X. Therefore, we can use the linear expression obtained by its first-order Taylor expansion as the lower bound of $f(X)$ at the local point $X^{(i)}$, which can be written as

$$f(X) \geq f^{lb}(X) = f(X^{(i)}) + f'(X^{(i)})(X - X^{(i)}) \tag{64}$$

Appendix B
Proof of Lemma 2

Let $R(\mathbf{W}^{(i)}, \mathbf{P}^{(i)}, \mathbf{L}^{(i)})$ be the objective value of problem (23) in the i-th iteration for $i \geq 1$. Let $R_\omega(\mathbf{W}^{(i)}, \mathbf{P}^{(i)}, \mathbf{L}^{(i)})$ be the objective value of problems (24). Then, in the step 2 of the Algorithm 2, we can get the inequality as

$$R(\mathbf{W}^{(i-1)}, \mathbf{P}^{(i-1)}, \mathbf{L}^{(i-1)}) \overset{(e1)}{\leq} R_\omega(\mathbf{W}^{(i)}, \mathbf{P}^{(i-1)}, \mathbf{L}^{(i-1)}) \tag{65}$$

where equation $(e1)$ holds because the problem is convex and can be solved optimally.

Similarly, let $R_p^{lb}(\mathbf{W}^{(i)}, \mathbf{L}^{(i)}, \mathbf{A}^{(i)}, \hat{\mathbf{P}}^{(i)})$ be the lower bound objective value of problem (25). Likewise, in the step 3 of the Algorithm 2, we can get the inequality as

$$\begin{aligned} &R(\mathbf{W}^{(i-1)}, \mathbf{L}^{(i-1)}, \mathbf{P}^{(i-1)}) \\ &\overset{(e2)}{=} R_p^{lb}(\mathbf{W}^{(i-1)}, \mathbf{L}^{(i-1)}, \mathbf{A}^{(i-1)}, \hat{\mathbf{P}}^{(i-1)}) && \text{(66a)} \\ &\overset{(e1)}{\leq} R_p^{lb}(\mathbf{W}^{(i-1)}, \mathbf{L}^{(i-1)}, \mathbf{A}^{(i)}, \hat{\mathbf{P}}^{(i)}) && \text{(66b)} \\ &\overset{(e3)}{\leq} R(\mathbf{W}^{(i-1)}, \mathbf{L}^{(i-1)}, \mathbf{P}^{(i)}) && \text{(66c)} \end{aligned}$$

where equation $(e2)$ holds because the first-order Taylor expansions are tight; equation $(e3)$ holds because the objective value is a lower bound of the original problem

Additionally, let $R_l^{lf}(\mathbf{W}^{(i)}, \mathbf{P}^{(i)}, \mathbf{L}^{(i)})$ be the replacement function of problem (36), and let $R_l^{lb}(\mathbf{W}^{(i)}, \mathbf{P}^{(i)}, \mathbf{L}^{(i)})$ be the lower bound objective value of problems (36). Likewise, in the step 4 of the Algorithm 2, we can get the inequality as

$$\begin{aligned} &R(\mathbf{W}^{(i-1)}, \mathbf{P}^{(i-1)}, \mathbf{L}^{(i-1)}) \\ &\overset{(e2)}{=} R_l^{lb}(\mathbf{W}^{(i-1)}, \mathbf{P}^{(i-1)}, \mathbf{L}^{(i-1)}) && \text{(67a)} \\ &\overset{(e1)}{\leq} R_l^{lb}(\mathbf{W}^{(i-1)}, \mathbf{P}^{(i-1)}, \mathbf{L}^{(i)}) && \text{(67b)} \\ &\overset{(e4)}{\leq} R_l^{lf}(\mathbf{W}^{(i-1)}, \mathbf{P}^{(i-1)}, \mathbf{L}^{(i)}) && \text{(67c)} \\ &\overset{(e2)}{=} R(\mathbf{W}^{(i-1)}, \mathbf{P}^{(i-1)}, \mathbf{L}^{(i)}) && \text{(67d)} \end{aligned}$$

where equation $(e4)$ holds because the introduction of smaller auxiliary variables.

Hence, from (65), (66) and (67), we further have

$$R(\mathbf{W}^{(i-1)}, \mathbf{P}^{(i-1)}, \mathbf{L}^{(i-1)}) \leq R(\mathbf{W}^{(i)}, \mathbf{P}^{(i)}, \mathbf{L}^{(i)}) \tag{68}$$

This is a peer-reviewed, accepted manuscript of the following paper: Liu, Z., Liu, X., Liu, Y., Leung, V. C. M., & Durrani, T. S. (2024). UAV assisted integrated sensing and communications for Internet of Things: 3D trajectory optimization and resource allocation. IEEE Transactions on Wireless Communications. Advance online publication. https://doi.org/10.1109/TWC.2024.3352985

which means that the objective function in (23) is non-decreasing after each iteration. Due to the objective value of problem (23) is finite, the Algorithm 2 is guaranteed to converge.

REFERENCES

[1] L. Zhao, G. Han, Z. Li and L. Shu, "Intelligent Digital Twin-Based Software-Defined Vehicular Networks," *IEEE Network*, vol. 34, no. 5, pp. 178-184, September/October 2020.

[2] D. C. Nguyen *et al.*, "6G Internet of Things: A Comprehensive Survey," *IEEE Internet of Things Journal*, vol. 9, no. 1, pp. 359-383, Jan, 2022.

[3] M. P. Singh and P. K. Murukannaiah, "Toward an Ethical Framework for Smart Cities and the Internet of Things," *IEEE Internet Computing*, vol. 27, no. 2, pp. 51-56, 1 March-April 2023.

[4] S. Feng and S. Haykin, "Cognitive Dynamic System for Future RACE Vehicles in Smart Cities: A Risk Control Perspective," *IEEE Internet of Things Magazine*, vol. 2, no. 1, pp. 14-20, March 2019.

[5] X. Yuan, J. Chen, N. Zhang, X. Fang and D. Liu, "A federated bidirectional connection broad learning scheme for secure data sharing in Internet of Vehicles" *China Communications*, vol. 18, no. 7, pp. 117-133, July 2021.

[6] H. Zhou, S. Pal, Z. Jadidi and A. Jolfaei, "A Fog-Based Security Framework for Large-Scale Industrial Internet of Things Environments," *IEEE Internet of Things Magazine*, vol. 6, no. 1, pp. 64-68, March 2023..

[7] W. Huang, T. Song and J. An, "QA2: QoS-Guaranteed Access Assistance for Space-Air-Ground Internet of Vehicle Networks," *IEEE Internet of Things Journal*, vol. 9, no. 8, pp. 5684-5695, 15 April, 2022.

[8] X. Liu, B. Lai, B. Lin and V. C. M. Leung, "Joint Communication and Trajectory Optimization for Multi-UAV Enabled Mobile Internet of Vehicles," *IEEE Transactions on Intelligent Transportation Systems*, vol. 23, no. 9, pp. 15354-15366, Sept. 2022.

[9] W. Wang, N. Zhao, L. Chen, X. Liu, Y. Chen and D. Niyato, "UAV-Assisted Time-Efficient Data Collection via Uplink NOMA," *IEEE Transactions on Communications*, vol. 69, no. 11, pp. 7851-7863, Nov. 2021.

[10] Z. Liu, X. Liu, V. C. M. Leung and T. S. Durrani, "Energy-Efficient Resource Allocation for Dual-NOMA-UAV Assisted Internet of Things," *IEEE Transactions on Vehicular Technology*, vol. 72, no. 3, pp. 3532-3543, March 2023.

[11] J. Liu, Y. Shi, Z. M. Fadlullah and N. Kato, "Space-Air-Ground Integrated Network: A Survey," *IEEE Communications Surveys & Tutorials*, vol. 20, no. 4, pp. 2714-2741, Fourthquarter 2018.

[12] Z. Feng, Z. Fang, Z. Wei, X. Chen, Z. Quan and D. Ji, "Joint radar and communication: A survey," *China Communications*, vol. 17, no. 1, pp. 1-27, Jan. 2020.

[13] Y. Cui, F. Liu, X. Jing and J. Mu, "Integrating Sensing and Communications for Ubiquitous IoT: Applications, Trends, and Challenges," *IEEE Network*, vol. 35, no. 5, pp. 158-167, September/October 2021.

[14] F. Liu *et al.*, "Integrated Sensing and Communications: Toward Dual-Functional Wireless Networks for 6G and Beyond," *IEEE Journal on Selected Areas in Communications*, vol. 40, no. 6, pp. 1728-1767, June 2022.

[15] J. A. Zhang et al., "Enabling Joint Communication and Radar Sensing in Mobile Networks : A Survey," *IEEE Communications Surveys & Tutorials*, vol. 24, no. 1, pp. 306-345, Firstquarter 2022.

[16] A. R. Chiriyath, B. Paul, G. M. Jacyna and D. W. Bliss, "Inner Bounds on Performance of Radar and Communications Co-Existence," *IEEE Transactions on Signal Processing*, vol. 64, no. 2, pp. 464-474, Jan.15, 2016.

[17] F. Liu, L. Zhou, C. Masouros, A. Li, W. Luo and A. Petropulu, "Toward Dual-functional Radar-Communication Systems: Optimal Waveform Design," *IEEE Transactions on Signal Processing*, vol. 66, no. 16, pp. 4264-4279, 15 Aug.15, 2018.

[18] Z. Xiao and Y. Zeng, "Waveform Design and Performance Analysis for Full-Duplex Integrated Sensing and Communication," *IEEE Journal on Selected Areas in Communications*, vol. 40, no. 6, pp. 1823-1837, June 2022.

[19] J. A. Zhang, X. Huang, Y. J. Guo, J. Yuan and R. W. Heath, "Multibeam for Joint Communication and Radar Sensing Using Steerable Analog Antenna Arrays," *IEEE Transactions on Vehicular Technology*, vol. 68, no. 1, pp. 671-685, Jan. 2019.

[20] L. Zhao, D. Wu, L. Zhou and Y. Qian, "Radio Resource Allocation for Integrated Sensing, Communication, and Computation Networks," *IEEE Transactions on Wireless Communications*, vol. 21, no. 10, pp. 8675-8687, Oct. 2022.

[21] N. Zhao, Y. Wang, Z. Zhang, Q. Chang and Y. Shen, "Joint Transmit and Receive Beamforming Design for Integrated Sensing and Communication," *IEEE Communications Letters*, vol. 26, no. 3, pp. 662-666, March 2022.

[22] W. Yuan, Z. Wei, S. Li, J. Yuan and D. W. K. Ng, "Integrated Sensing and Communication-Assisted Orthogonal Time Frequency Space Transmission for Vehicular Networks," *IEEE Journal of Selected Topics in Signal Processing*, vol. 15, no. 6, pp. 1515-1528, Nov. 2021.

[23] J. Mu, Y. Gong, F. Zhang, Y. Cui, F. Zheng and X. Jing, "Integrated Sensing and Communication-Enabled Predictive Beamforming With Deep Learning in Vehicular Networks," *IEEE Communications Letters*, vol. 25, no. 10, pp. 3301-3304, Oct. 2021.

[24] Q. Zhang, X. Wang, Z. Li and Z. Wei, "Design and Performance Evaluation of Joint Sensing and Communication Integrated System for 5G mmWave Enabled CAVs," *IEEE Journal of Selected Topics in Signal Processing*, vol. 15, no. 6, pp. 1500-1514, Nov. 2021.

[25] Q. Zhang, H. Sun, X. Gao, X. Wang and Z. Feng, "Time-division ISAC Enabled Connected Automated Vehicles Cooperation Algorithm Design and Performance Evaluation," *IEEE Journal on Selected Areas in Communications*, 2022, to appear.

[26] W. Jiang *et al.*, "Improve Sensing and Communication Performance of UAV via Integrated Sensing and Communication," *2021 IEEE 21st International Conference on Communication Technology (ICCT)*, 2021, pp. 644-648.

[27] B. Chang, W. Tang, X. Yan, X. Tong and Z. Chen, "Integrated Scheduling of Sensing, Communication, and Control for mmWave/THz Communications in Cellular Connected UAV Networks," *IEEE Journal on Selected Areas in Communications*, vol. 40, no. 7, pp. 2103-2113, July 2022.

[28] X. Wang, Z. Fei, J. A. Zhang, J. Huang and J. Yuan, "Constrained Utility Maximization in Dual-Functional Radar-Communication Multi-UAV Networks," *IEEE Transactions on Communications*, vol. 69, no. 4, pp. 2660-2672, April 2021.

[29] X. Chen, Z. Feng, Z. Wei, F. Gao and X. Yuan, "Performance of Joint Sensing-Communication Cooperative Sensing UAV Network," *IEEE Transactions on Vehicular Technology*, vol. 69, no. 12, pp. 15545-15556, Dec. 2020.

[30] K. Zhang and C. Shen, "UAV Aided Integrated Sensing and Communications," *2021 IEEE 94th Vehicular Technology Conference (VTC2021-Fall)*, 2021, pp. 1-6.

[31] S. Zhang, H. Zhang, Z. Han, H. V. Poor and L. Song, "Age of Information in a Cellular Internet of UAVs: Sensing and Communication Trade-Off Design," *IEEE Transactions on Wireless Communications*, vol. 19, no. 10, pp. 6578-6592, Oct. 2020.

[32] S. Hu, X. Yuan, W. Ni and X. Wang, "Trajectory Planning of Cellular-Connected UAV for Communication-Assisted Radar Sensing," *IEEE Transactions on Communications*, vol. 70, no. 9, pp. 6385-6396, Sept. 2022.

[33] T. Zhang, K. Zhu, S. Zheng, D. Niyato and N. C. Luong, "Trajectory Design and Power Control for Joint Radar and Communication Enabled Multi-UAV Cooperative Detection Systems," *IEEE Transactions on Communications*, vol. 71, no. 1, pp. 158-172, Jan. 2023.

[34] K. Meng, Q. Wu, S. Ma, W. Chen, K. Wang and J. Li, "Throughput Maximization for UAV-Enabled Integrated Periodic Sensing and Communication," *IEEE Transactions on Wireless Communications*, vol. 22, no. 1, pp. 671-687, Jan. 2023.

[35] Y. Liu, S. Liu, X. Liu, Z. Liu and T. S. Durrani, "Sensing Fairness Based Energy Efficiency Optimization for UAV Enabled Integrated Sensing and Communication," *IEEE Wireless Communications Letters*, 2023 to appear.

[36] C. E. Shannon, "A mathematical theory of communication," Bell Syst. Tech. J., vol. 27, no. 3, pp. 379-423, Jul. 1948.

[37] A. R. Chiriyath, B. Paul and D. W. Bliss, "Radar-Communications Convergence: Coexistence, Cooperation, and Co-Design,"*IEEE Transactions on Cognitive Communications and Networking*, vol. 3, no. 1, pp. 1-12, March 2017.

[38] S. Zhang, J. Yang, H. Zhang and L. Song, "Dual Trajectory Optimization for a Cooperative Internet of UAVs,"*IEEE Communications Letters*, vol. 23, no. 6, pp. 1093-1096, June 2019.

[39] Y. Jin, H. Zhang, S. Zhang, Z. Han and L. Song, "Sense-Store-Send: Trajectory Optimization for a Buffer-Aided Internet of UAVs," *IEEE Communications Letters*, vol. 24, no. 12, pp. 2888-2892, Dec. 2020.

[40] Qualcomm Technologies, Inc.,"LTE unmanned aircraft systems, SanDiego, CA, USA, Trial report v.1.0.1, 2017.

[41] X. Lin et al., The Sky Is Not the Limit: LTE for Unmanned Aerial Vehicles, *IEEE Communications Magazine*, vol. 56, no. 4, pp. 204-210, April 2018.

This is a peer-reviewed, accepted manuscript of the following paper: Liu, Z., Liu, X., Liu, Y., Leung, V. C. M., & Durrani, T. S. (2024). UAV assisted integrated sensing and communications for Internet of Things: 3D trajectory optimization and resource allocation. IEEE Transactions on Wireless Communications. Advance online publication. https://doi.org/10.1109/TWC.2024.3352985

[42] T. S. Rappaport, Wireless Communications: Principles and Practice. Prentice Hall PTR, 1996.
[43] M. Richards, J. Scheer, W.Holm, Principles of modern radar: Basic principles. IET Digital Library, 2010.

Zechen Liu received the B.S. degree from Shandong Agricultural University, Taian, China, in 2019. He is currently working toward the Ph.D. degree with the School of Information and Communication Engineering, Dalian University of Technology, China. His research interests focus on UAV, integrated sensing and communications, non-orthogonal multiple access, Internet of Things and communication resource optimization.

Xin Liu (M'13-SM'19) received the M.Sc degree and the Ph.D. degree in Communication Engineering from the Harbin Institute of Technology in 2008 and 2012, respectively. He is currently an Associate Professor with the School of Information and Communication Engineering, Dalian University of Technology, China. From 2012 to 2013, he was a Research Fellow with the School of Electrical and Electronic Engineering, Nanyang Technological University, Singapore. From 2013 to 2016, he was a Lecturer with the College of Astronautics, Nanjing University of Aeronautics and Astronautics, China. His research interests focus on communication signal processing, cognitive radio, spectrum resource allocation and broadband satellite communications.

Yuemin Liu received his B.S degree in Communication Engineering, Liaoning University, China, in 2022. He is currently pursuing the M.S. degree with the School of Information and Communication Engineering, Dalian University of Technology, China. His current research interests focus on UAV trajectory optimization, Internet of Things, integrated sensing and communications, mobile communication and resource allocation.

Victor C. M. Leung (Life Fellow, IEEE) is a Distinguished Professor of Computer Science and Software Engineering at Shenzhen University, China. He is also an Emeritus Professor of Electrical and Computer Engineering and Director of the Laboratory for Wireless Networks and Mobile Systems at the University of British Columbia (UBC), Canada. His research is in the broad areas of wireless networks and mobile systems, and he has published widely in these areas. Dr. Leung is serving on the editorial boards of the IEEE Transactions on Green Communications and Networking, IEEE Transactions on Cloud Computing, IEEE Transactions on Computational Social Systems, IEEE Access, IEEE Network, and several other journals. He received the 1977 APEBC Gold Medal, 1977-1981 NSERC Postgraduate Scholarships, IEEE Vancouver Section Centennial Award, 2011 UBC Killam Research Prize, 2017 Canadian Award for Telecommunications Research, 2018 IEEE TCGCC Distinguished Technical Achievement Recognition Award, and 2018 ACM MSWiM Reginald Fessenden Award. He co-authored papers that won the 2017 IEEE ComSoc Fred W. Ellersick Prize, 2017 IEEE Systems Journal Best Paper Award, 2018 IEEE CSIM Best Journal Paper Award, and 2019 IEEE TCGCC Best Journal Paper Award. He is a Fellow of the Royal Society of Canada (Academy of Science), Canadian Academy of Engineering, and Engineering Institute of Canada. He is named in the current Clarivate Analytics list of Highly Cited Researchers.

Tariq S. Durrani (Life Fellow, IEEE) is a Full Professor with the University of Strathclyde, Scotland, UK, where he was Deputy Principal of the University from 2000-06. He is Past Vice President of the Royal Society of Edinburgh and the IEEE, Past President of the IEEE Signal Processing Society and the IEEE Engineering Management Society. He has been the General Chair of several flagship international conferences, including IEEE ICASSP-89, Transputers-91, IEEE IEMC-02, European Universities Convention-2006, and IEEE ICC-07. He is a Fellow of the Royal Academy of Engineering, UK, the Royal Society of Edinburgh, UK, the National Academy of Sciences, USA, and the IEEE. His research interests include statistical signal and image processing, technology management, and higher education management.

This is a peer-reviewed, accepted manuscript of the following paper: Liu, Z., Liu, X., Liu, Y., Leung, V. C. M., & Durrani, T. S. (2024). UAV assisted integrated sensing and communications for Internet of Things: 3D trajectory optimization and resource allocation. IEEE Transactions on Wireless Communications. Advance online publication. https://doi.org/10.1109/TWC.2024.3352985